



Cite this: *Mol. Syst. Des. Eng.*, 2023, 8, 431

Received 26th December 2022,  
Accepted 13th February 2023

DOI: 10.1039/d2me00277a

rsc.li/molecular-engineering

To realize lanthanide metal-organic frameworks (Ln-MOFs) with white light emission, it is necessary to adjust their RGB composition. We adopted the Bayesian optimization technique to optimize the stoichiometric ratio of metal-salts in Ln-MOFs. We successfully synthesized MIL-103 ( $\text{Ln}(\text{BTB})(\text{H}_2\text{O})$ ,  $\text{H}_3\text{BTB} = 1,3,5\text{-tris}(4\text{-carboxyphenyl})\text{benzene}$ ), which emits white light.

Lanthanide-based metal-organic frameworks (Ln-MOFs) have gained significant attention in recent years because of their potential for use as multifunctional materials, including luminescent materials, sensors, proton conductors, and magnetic materials.<sup>1–8</sup> Ln-MOFs are excellent luminescent materials because they can be freely tuned to various luminescence colors by mixing an appropriate amount of lanthanide metal ions. Furthermore, they can be used in diverse applications such as displays, image processing, and color barcodes.<sup>9–11</sup> Ln-MOFs can cover the three primary color emissions (RGB; red, green, and blue), which allows their application in the design of materials with white light emission.<sup>12–14</sup> However, controlling the emission color of Ln-MOFs can be challenging because energy is generally transferred from blue-emission chromophores to green-emission chromophores and from green-emission chromophores to red-emission chromophores, which is a complex process.<sup>15–17</sup> Commercial lanthanide reagents contain trace amounts of other lanthanide metals,<sup>18</sup> and the presence of  $\text{Eu}^{3+}$ , a red-emission chromophore, as an impurity has a significant impact on the luminescence properties of such reagents because excess energy transfer to  $\text{Eu}^{3+}$  results in reddish luminescence.<sup>19</sup> Therefore, predicting the composition necessary to achieve the desired

## Bayesian optimization of the composition of the lanthanide metal-organic framework MIL-103 for white-light emission†

Yu Kitamura,<sup>a</sup> Hiroki Toshima,<sup>a</sup> Akihiro Inokuchi<sup>b</sup> and Daisuke Tanaka   

### Design, System, Application

This study provides an approach to efficiently optimize the composition of the lanthanide-based metal-organic framework (MOF) MIL-103, which shows white light emission, by adopting the Bayesian optimization method. Predicting the lanthanide ion composition that can result in the desired luminescence color is often difficult because it requires rigorous experimentation based on intuition and experience. The use of Bayesian optimization methods for composition optimization can help resolve the problems associated with complex energy transfer processes and the presence of trace amounts of lanthanide impurities. The proposed approach is an effective means to overcome the challenges of compositional optimization beyond the limitations of the experimenter. We successfully synthesized white-light-emitting MIL-103 using Bayesian optimization. The field of material informatics (MI) has gained significant attention, and a versatile method based on MI for composite optimization of MOFs is desired, as a limited number of studies have reported the application of machine learning to synthesize MOFs.

Published on 14/2023. Downloaded on 06/02/2026 06:40:29.

luminescence color is often difficult because it requires numerous experiments based on intuition and experience.

In recent years, the field of material informatics has gained significant attention and has been actively studied to facilitate the discovery of novel materials.<sup>18,20–29</sup> In particular, Bayesian optimization predicts an unknown function and suggests the next search condition where the probability of showing a maximum or minimum value is high.<sup>30</sup> Bayesian optimization methods are useful tools for yield improvement and composition optimization.<sup>31–41</sup> The use of Bayesian optimization methods for composition optimization could help resolve the problems associated with the complex energy transfer and trace amounts of lanthanide impurities in Ln-MOFs. Bayesian optimization searches for conditions that help achieve white luminescence properties using the amount of rare earth salts in the raw material as a parameter, eliminating the need for the experimenter to directly consider

<sup>a</sup> Department of Chemistry, School of Science, Kwansei Gakuin University, 1 Gakuen-Uegahara, Sanda, Hyogo 669-1337, Japan. E-mail: dtanaka@kwansei.ac.jp

<sup>b</sup> Program of Computer Science, School of Engineering, Kwansei Gakuin University, 1 Gakuen-Uegahara, Sanda, Hyogo 669-1337, Japan

† Electronic supplementary information (ESI) available. See DOI: <https://doi.org/10.1039/d2me00277a>

the amount of impurities and the efficiency of energy transfer.

Herein, we focused on MIL-103 ( $\text{Ln}(\text{BTB})(\text{H}_2\text{O})$ , BTB = 1,3,5-tris(4-carboxyphenyl)benzene), which has been reported to be synthesized with various lanthanide ions.<sup>42</sup> The primary objective of the study was to optimize the composition of MIL-103, which shows white light emission, by adopting the Bayesian optimization method (Fig. 1). However, in order to perform Bayesian optimization, a large initial data set is required. Therefore, in this study, synthesis was performed using multiple reaction vessels that can collect a large amount of data at a time, and fluorescence spectra were collected using a microplate reader.

MIL-103 ( $\text{Ln} = \text{Eu}^{3+}$ ,  $\text{Gd}^{3+}$ ,  $\text{Tb}^{3+}$ ) was synthesized using the solvothermal method, wherein three different lanthanide metals,  $\text{Eu}^{3+}$ ,  $\text{Gd}^{3+}$ , and  $\text{Tb}^{3+}$  were used, following a previously reported synthetic method.<sup>42</sup> The successful synthesis of MIL-103 was confirmed through X-ray powder diffraction (XRPD; Fig. S1†). The luminescence spectra of these three materials were recorded, and chromaticity diagrams were prepared accordingly; MIL-103(Eu) and MIL-103(Tb) emitted red and green luminescence, respectively, as expected (Fig. 2a-d and S2†). However, MIL-103(Gd), which was expected to show light blue luminescence from the ligand, showed light purple luminescence. Thus, we recorded the luminescence spectrum of the ligand,  $\text{H}_3\text{BTB}$ , and found that  $\text{H}_3\text{BTB}$  emits blue luminescence (Fig. 2c). In addition to the expected band from  $\text{H}_3\text{BTB}$ , the luminescence spectrum

of MIL-103(Gd) showed peaks which can be attributed to Eu-derived peaks. This further indicates that the impurity  $\text{Eu}^{3+}$  was included in MIL-103(Gd) (Fig. 2c). To identify the origin of the impurity  $\text{Eu}^{3+}$ , we focused on the starting material, the  $\text{Gd}^{3+}$  nitrate salt. In our previous work,<sup>18</sup> we performed inductively coupled plasma mass spectrometry measurements and demonstrated that  $\text{Tb}(\text{NO}_3)_3 \cdot 6\text{H}_2\text{O}$  contained 0.2% Eu and  $\text{Gd}(\text{NO}_3)_3 \cdot 6\text{H}_2\text{O}$  contained 0.1% Eu and Tb. These impurity ions endow light purple luminescence to MIL-103(Gd). These results indicate that, to synthesize MIL-103 with white light emission, only a small amount of Eu is required primarily because of the presence of Eu in the Gd and Tb precursors.

To realize white light emission,  $\text{MIL-103}(\text{Eu}_x\text{Gd}_y\text{Tb}_z)$  was synthesized according to various metal ion mixing ratios. The concentration ratio was determined based on the intuition and experience of the experimenter. A total of 156 different conditions were investigated over six trials (Table S1†). The obtained products were characterized by XRPD, luminescence spectra were measured under a 295 nm excitation wavelength, and the corresponding chromaticity diagram data were collected (Fig. 2e). In the first trial, only red luminescence was obtained. As the number of trials increased, orange luminescence and pink luminescence were obtained gradually. However, in this screening, the CIE chromaticity coordinates closest to white were (0.372, 0.308) at the changed ratio of  $\text{MIL-103}(\text{Eu}_x\text{Gd}_y\text{Tb}_z)$ ;  $\text{Eu} = 2.7 \times 10^{-5}$ ,  $\text{Tb} = 5.6 \times 10^{-3}$ ,  $\text{Gd} = 9.94 \times 10^{-1}$ , which shows light-pink emission, while the ideal white emission CIE coordinates were (0.333, 0.333), i.e., we could not obtain white-light emitting products (Fig. 2e and S3 and S4†).

The initial screening synthesis could not yield MIL-103 with white-light emission under an excitation wavelength of 295 nm. It is known that the luminescence spectrum of lanthanide compounds is dependent on the excitation wavelength. Therefore, we performed tuning experiments by varying the excitation wavelengths in the range 250–310 nm. Thus, nearly white light emission (0.327, 0.340) was successfully obtained at an excitation wavelength of 250 nm when the metal ions (Eu, Gd, and Tb) were added at a concentration ratio of  $8.3 \times 10^{-5} : 9.92 \times 10^{-1} : 8.1 \times 10^{-3}$ ; i.e. when  $\text{MIL-103}(\text{Eu}_x\text{Gd}_y\text{Tb}_z)$ ;  $\text{Eu} = 8.3 \times 10^{-5}$ ,  $\text{Tb} = 8.1 \times 10^{-3}$ ,  $\text{Gd} = 9.92 \times 10^{-1}$  was prepared (Fig. 3).

To synthesize white-light emitting MIL-103 under a longer excitation wavelength, we tried to optimize the composition of the lanthanide metal contents using a Bayesian optimization technique. For the purpose of analysis, the 156 chromaticity coordinate data collected in the initial screening and synthetic conditions for the lanthanide metal mixing ratio were used. The distance between the white color (0.333, 0.333) and the chromaticity diagram coordinates obtained using the screening synthesis was calculated (eqn (1)), and Bayesian optimization was performed to minimize this distance to “0.”

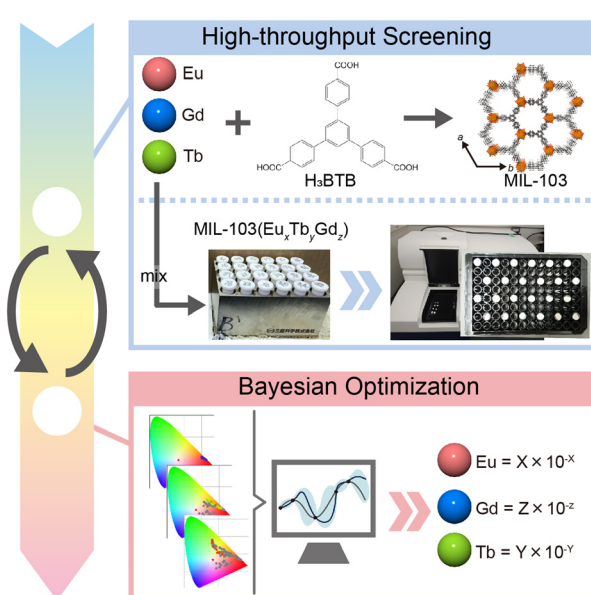


**Fig. 1** Research flow process. Data were collected by changing the stoichiometric ratio of the three lanthanide metal-salts and conducting 24 or 48 variations six times using multiple reaction vessels. Fluorescence measurements were performed using microplate readers to collect 24 spectra at a time. Based on the data, Bayesian optimization was performed to optimize the stoichiometric ratio that shows white-light emission.

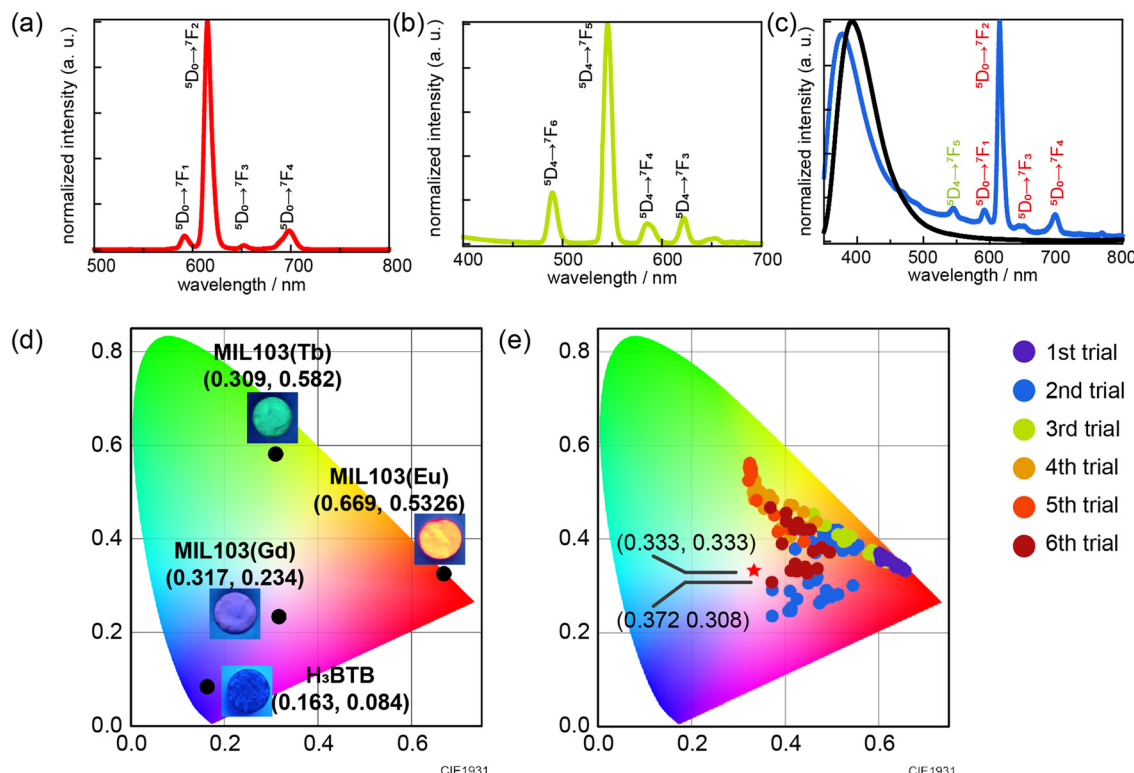


Fig. 2 Emission spectra at an excitation wavelength of 295 nm: (a) single MIL-103(Eu), (b) single MIL-103(Tb), and (c) single MIL-103(Gd) (blue) and organic ligand H<sub>3</sub>BTB (black). (d) CIE chromaticity diagram for single MIL-103(Eu, Gd, or Tb) and organic ligand H<sub>3</sub>BTB. (e) CIE chromaticity diagram for trial experiments 1–6.

$$\text{Distance} = \sqrt{(x_i - 0.333)^2 + (y_i - 0.333)^2} \quad (1)$$

( $x_i$ : x-coordinate of any chromaticity diagram,  $y_i$ : y-coordinate of any chromaticity diagram)

The Bayesian optimization yielded an optimized amount of Eu(NO<sub>3</sub>)<sub>3</sub>·6H<sub>2</sub>O = 9.90 × 10<sup>-7</sup>, Tb(NO<sub>3</sub>)<sub>3</sub>·6H<sub>2</sub>O = 1.96 × 10<sup>-4</sup>, and Gd(NO<sub>3</sub>)<sub>3</sub>·6H<sub>2</sub>O = 3.75 × 10<sup>-2</sup> mmol for each lanthanide metal salt. Based on this information on the optimized preparation ratio, 10 synthetic conditions were examined (Table S2†). We characterized the obtained powder *via* XRPD.

We then measured luminescence spectra and subsequently generated chromaticity coordinates. Although we could not obtain white color emission in the initial screening synthesis, all the MIL-103 samples synthesized according to Bayesian optimization successfully yielded near-white-light emission (Fig. 4b and c and S5 and S6†). The closest white-light emission was achieved for MIL-103(Eu<sub>x</sub>Gd<sub>y</sub>Tb<sub>z</sub>; Eu = 2.9 × 10<sup>-5</sup>, Tb = 5.1 × 10<sup>-3</sup>, Gd = 9.95 × 10<sup>-1</sup>), which showed white-light emission with (0.332, 0.341) under 295 nm excitation (Fig. 4a). Though the experimenter could not obtain white luminescence by intuition and experience, the desired

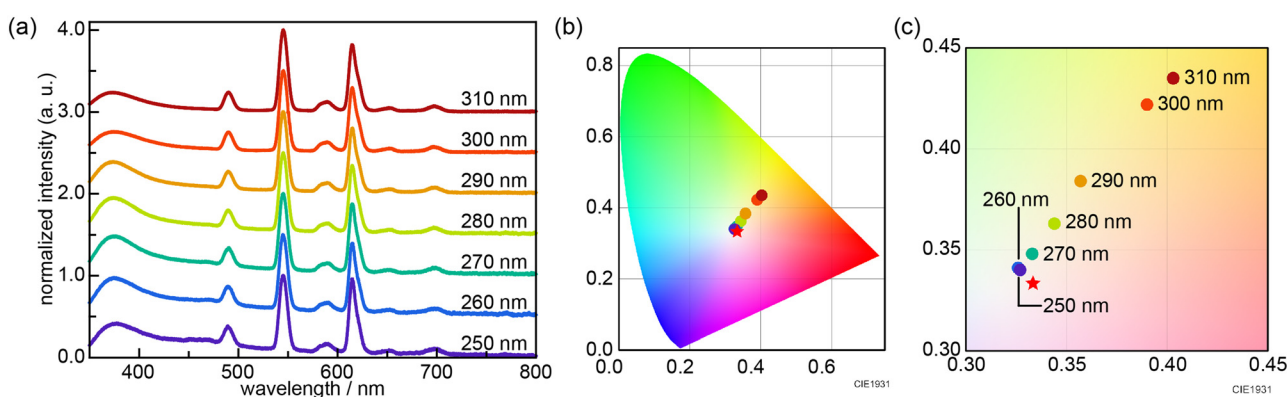
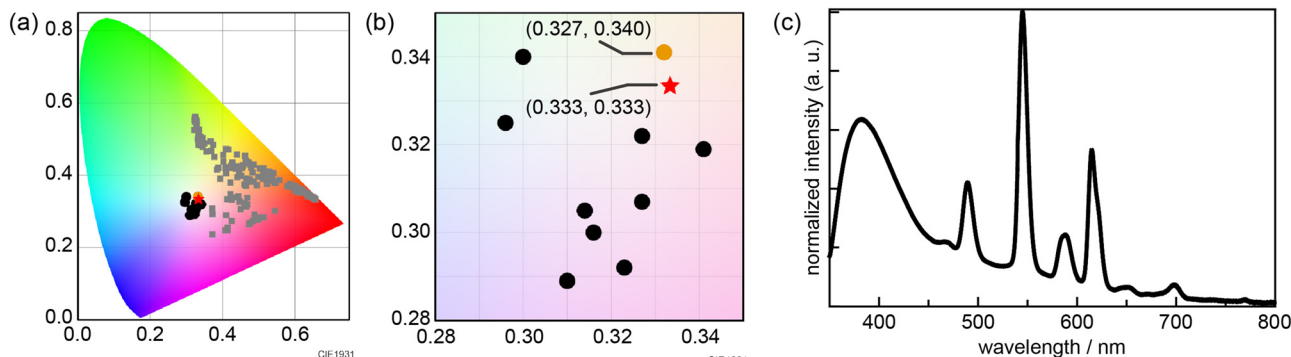


Fig. 3 (a) Emission spectra and (b) CIE chromaticity diagram of MIL-103(Eu<sub>x</sub>Gd<sub>y</sub>Tb<sub>z</sub>; Eu = 8.3 × 10<sup>-5</sup>, Tb = 8.1 × 10<sup>-3</sup>, Gd = 9.92 × 10<sup>-1</sup>) at various excitation wavelengths. (c) Enlarged view of Fig. 3b.



**Fig. 4** (a) CIE chromaticity diagram after Bayesian optimization. The red star is the white color (0.333, 0.333). The circles are the experimental results with the lanthanide metal content optimized using Bayesian optimization. The orange circle is the result closest to white-light emission (0.332, 0.341). The gray squares are the results from the initial screening synthesis. (b) Enlarged view of Fig. 4b. (c) Emission spectrum of white-light emission of  $\text{MIL-103}(\text{Eu}_x\text{Gd}_y\text{Tb}_z$ ;  $\text{Eu} = 2.9 \times 10^{-5}$ ,  $\text{Tb} = 5.1 \times 10^{-5}$ ,  $\text{Gd} = 9.95 \times 10^{-3}$ ). The excitation wavelength was 295 nm.

luminescence could be successfully achieved based on the results of Bayesian optimization.

In summary, we successfully synthesized white-light-emitting MIL-103 using two different approaches: adjusting the excitation wavelength and optimizing the lanthanide metal content using Bayesian optimization. The initial screening synthesis was performed by relying on the intuition and experience of the experimenter. Although the experimenter's intuition was cultivated as the number of trials increased, it was difficult to synthesize white-light-emitting MIL-103. Meanwhile, the composition of lanthanide metals in MIL-103 could be optimized efficiently through Bayesian optimization. Thus, this method is an effective means to overcome the challenges of composition optimization beyond the limitations of the experimenter and is expected to facilitate material discovery.

This work was supported by JSPS KAKENHI (Grant No. 20H02577), JST PRESTO (grant no. JPMJPR17NA), the Sasakawa Scientific Research Grant from The Japan Science Society, and the FY2022 Individual Special Research Fund from KG University. We thank Editage (<https://www.edition.com/>) for English language editing.

## Conflicts of interest

There are no conflicts to declare.

## References

- J. Rocha, L. D. Carlos, F. A. Paz and D. Ananias, *Chem. Soc. Rev.*, 2011, **40**, 926–940.
- J. Heine and K. Muller-Buschbaum, *Chem. Soc. Rev.*, 2013, **42**, 9232–9242.
- L. V. Meyer, F. Schonfeld and K. Muller-Buschbaum, *Chem. Commun.*, 2014, **50**, 8093–8108.
- S. Roy, A. Chakraborty and T. K. Maji, *Coord. Chem. Rev.*, 2014, **273–274**, 139–164.
- W. P. Lustig, S. Mukherjee, N. D. Rudd, A. V. Desai, J. Li and S. K. Ghosh, *Chem. Soc. Rev.*, 2017, **46**, 3242–3285.
- X. Meng, H. N. Wang, S. Y. Song and H. J. Zhang, *Chem. Soc. Rev.*, 2017, **46**, 464–480.
- D. W. Lim and H. Kitagawa, *Chem. Rev.*, 2020, **120**, 8416–8467.
- F. Saraci, V. Quezada-Novoa, P. R. Donnarumma and A. J. Howarth, *Chem. Soc. Rev.*, 2020, **49**, 7949–7977.
- K. A. White, D. A. Chengelis, K. A. Gogick, J. Stehman, N. L. Rosi and S. Petoud, *J. Am. Chem. Soc.*, 2009, **131**, 18069–18071.
- Y. Lu and B. Yan, *J. Mater. Chem. C*, 2014, **2**, 7411–7416.
- Q. Y. Yang, M. Pan, S. C. Wei, K. Li, B. B. Du and C. Y. Su, *Inorg. Chem.*, 2015, **54**, 5707–5716.
- X. Ma, X. Li, Y.-E. Cha and L.-P. Jin, *Cryst. Growth Des.*, 2012, **12**, 5227–5232.
- Q. Tang, S. Liu, Y. Liu, D. He, J. Miao, X. Wang, Y. Ji and Z. Zheng, *Inorg. Chem.*, 2014, **53**, 289–293.
- Y. W. Zhao, F. Q. Zhang and X. M. Zhang, *ACS Appl. Mater. Interfaces*, 2016, **8**, 24123–24130.
- Y. Cui, B. Chen and G. Qian, *Coord. Chem. Rev.*, 2014, **273–274**, 76–86.
- Y. Hirai, T. Nakanishi, K. Miyata, K. Fushimi and Y. Hasegawa, *Mater. Lett.*, 2014, **130**, 91–93.
- J. Rocha, C. D. Brites and L. D. Carlos, *Chem. – Eur. J.*, 2016, **22**, 14782–14795.
- Y. Kitamura, E. Terado, Z. Zhang, H. Yoshikawa, T. Inose, I. H. Uji, M. Tanimizu, A. Inokuchi, Y. Kamakura and D. Tanaka, *Chem. – Eur. J.*, 2021, **27**, 16347–16353.
- E. G. Moore, A. P. S. Samuel and K. N. Raymond, *Acc. Chem. Res.*, 2009, **42**, 542–552.
- P. Raccuglia, K. C. Elbert, P. D. Adler, C. Falk, M. B. Wenny, A. Mollo, M. Zeller, S. A. Friedler, J. Schrier and A. J. Norquist, *Nature*, 2016, **533**, 73–76.
- V. Duros, J. Grizou, W. Xuan, Z. Hosni, D. L. Long, H. N. Miras and L. Cronin, *Angew. Chem., Int. Ed.*, 2017, **56**, 10815–10820.
- V. Duros, J. Grizou, A. Sharma, S. H. M. Mehr, A. Bubliauskas, P. Frei, H. N. Miras and L. Cronin, *J. Chem. Inf. Model.*, 2019, **59**, 2664–2671.

23 S. M. Moosavi, A. Chidambaram, L. Talirz, M. Haranczyk, K. C. Stylianou and B. Smit, *Nat. Commun.*, 2019, **10**, 1–7.

24 K. Muraoka, Y. Sada, D. Miyazaki, W. Chaikittisilp and T. Okubo, *Nat. Commun.*, 2019, **10**, 1–12.

25 X. Yang, Y. Wang, R. Byrne, G. Schneider and S. Yang, *Chem. Rev.*, 2019, **119**, 10520–10594.

26 K. M. Jablonka, D. Ongari, S. M. Moosavi and B. Smit, *Chem. Rev.*, 2020, **120**, 8066–8129.

27 S. M. Moosavi, K. M. Jablonka and B. Smit, *J. Am. Chem. Soc.*, 2020, **142**, 20273–20287.

28 Y. Xie, C. Zhang, X. Hu, C. Zhang, S. P. Kelley, J. L. Atwood and J. Lin, *J. Am. Chem. Soc.*, 2020, **142**, 1475–1481.

29 T. Wakiya, Y. Kamakura, H. Shibahara, K. Ogasawara, A. Saeki, R. Nishikubo, A. Inokuchi, H. Yoshikawa and D. Tanaka, *Angew. Chem., Int. Ed.*, 2021, **60**, 23217–23224.

30 T. Ueno, T. D. Rhone, Z. Hou, T. Mizoguchi and K. Tsuda, *Materials Discovery*, 2016, **4**, 18–21.

31 T. Yamashita, N. Sato, H. Kino, T. Miyake, K. Tsuda and T. Oguchi, *Phys. Rev. Mater.*, 2018, **2**, 013803.

32 A. Deshwal, C. M. Simon and J. R. Doppa, *Mol. Syst. Des. Eng.*, 2021, **6**, 1066–1086.

33 B. J. Shields, J. Stevens, J. Li, M. Parasram, F. Damani, J. I. M. Alvarado, J. M. Janey, R. P. Adams and A. G. Doyle, *Nature*, 2021, **590**, 89–96.

34 C. B. Wahl, M. Aykol, J. H. Swisher, J. H. Montoya, S. K. Suram and C. A. Mirkin, *Sci. Adv.*, 2021, **7**, eabj5505.

35 H. Zhang, H. Fu, S. Zhu, W. Yong and J. Xie, *Acta Mater.*, 2021, **215**, 117118.

36 D. Bash, Y. Cai, V. Chellappan, S. L. Wong, X. Yang, P. Kumar, J. D. Tan, A. Abutaha, J. J. W. Cheng, Y. F. Lim, S. I. P. Tian, Z. Ren, F. Mekki-Berrada, W. K. Wong, J. Xie, J. Kumar, S. A. Khan, Q. Li, T. Buonassisi and K. Hippalgaonkar, *Adv. Funct. Mater.*, 2021, **31**, 2102606–2102618.

37 A. Dave, J. Mitchell, S. Burke, H. Lin, J. Whitacre and V. Viswanathan, *Nat. Commun.*, 2022, **13**, 1–9.

38 Y. Naito, M. Kondo, Y. Nakamura, N. Shida, K. Ishikawa, T. Washio, S. Takizawa and M. Atobe, *Chem. Commun.*, 2022, **58**, 3893–3896.

39 X. Li, G. Shan and C. H. Shek, *J. Mater. Sci. Technol.*, 2022, **103**, 113–120.

40 X. Li, G. Shan, J. Zhang and C.-H. Shek, *J. Mater. Chem. C*, 2022, **10**, 17291–17302.

41 T. Zhou, R. Gani and K. Sundmacher, *Engineering*, 2021, **7**, 1231–1238.

42 J. Duan, M. Higuchi, S. Horike, M. L. Foo, K. P. Rao, Y. Inubushi, T. Fukushima and S. Kitagawa, *Adv. Funct. Mater.*, 2013, **23**, 3525–3530.